Desalination 416 (2017) 106–121

Contents lists available at ScienceDirect

Desalination

journal homepage: www.elsevier.com/locate/desal

Experimental study on the effect of polysaccharides on incipient membrane scaling during desalination

A.J. Karabelas*, A. Karanasiou, D.C. Sioutopoulos

Laboratory of Natural Resources and Renewable Energies, Chemical Process and Energy Resources Institute, Centre for Research and Technology - Hellas, P.O. Box 60361, GR57001 Thermi, Thessaloniki, Greece

ARTICLE INFO

Keywords:
RO desalination of brackish-type
Membrane scaling in presence of alginates
Alginates in small concentration inhibit scaling

ABSTRACT

Experimental results are reported on the effect of polysaccharides in the early stage of membrane scaling. Sodium alginate at small concentration (2 and 10 mg/L) was employed as typical polysaccharide. Synthetic solutions, characterized by small bulk supersaturation ratio S in calcium sulfate (S ~ 1.4), were filtered through a desalination membrane in dead-end cells under agitation. Three types of tests were performed; i.e. membrane scaling in absence of alginates (as reference), combined fouling-scaling (i.e. scaling in presence of alginates) and scaling tests after a fouling layer was formed on the membrane. Examination of various deposits by Scanning Electron Microscopy (SEM) and determination of calcium on membrane deposits and in filtered solids (from retentate and feed-fluid samples) provide useful insights including clear evidence that alginates tend to inhibit $CaSO_4$ crystallization, likely due to calcium binding with carboxylates of alginate macromolecules and formation of gel deposits. The inhibition effect, manifested in the reduced deposit-mass density on membranes and crystallization–rate, as well as in crystal-shape modification, is stronger at the higher alginate concentration. Similarly, incipient membrane scaling, pretreated with alginate foulant solution, appears to be significantly inhibited compared to clean membranes. Under the conditions tested, membrane salt rejection was unaffected.

1. Introduction

The inherent problem of membrane performance deterioration due various deposited species (generally referred to as “membrane fouling”) is a key issue in optimizing the design and operation of reverse osmosis (RO) desalination plants. Despite the complexity of the problem, it is broadly recognized that the major fouling categories are *organic fouling*, *bio-fouling*, *scaling*, and *colloidal/particulate fouling* [1]. The former two categories are inter-related in that extracellular polymeric substances (EPS), notably polysaccharides produced by micro-organisms, are key organic compounds causing (even at relatively small concentration) organic fouling and serving as a conditioning-agent of solid surfaces and of membranes that facilitates bacteria attachment and biofouling [2,3]. Humic acids and proteins are two other significant categories of organic foulants [4,5]. Regarding membrane scaling by sparingly soluble salts, calcium compounds (i.e. calcium sulfate, carbonate and phosphate) are the most common scale-forming species in processed feed-waters; several other cations (i.e. Mg, Ba, Sr) also tend to form such scale due to precipitation/crystallization under favorable thermodynamic conditions [6]. Additionally, colloidal inorganic species of Fe, Si, Al, usually in the form of hydroxides are encountered in deposits on desalination membranes [7].

Each aforementioned category of “membrane fouling” during desalination has been studied separately quite extensively. Regarding *organic fouling*, the extensive work (partly reviewed in [8]) mainly involves humic acids (HA), polysaccharides, and proteins; Sodium Alginate (SA) and Bovine Serum Albumin (BSA) are frequently employed as typical foulants of the latter two categories [9]. The level of understanding regarding desalination membrane fouling by HA and SA (separately) is considered fair, although significant gaps exist ([8,10]); however, the *combined effect* of organic foulants has been studied to a much lesser extent.

Scaling of solid impermeable surfaces by calcium salts (in the absence of organic matter) has been the topic of extensive investigation for more than 30 years, with a plethora of studies addressing the various issues related to solid phase nucleation, crystal growth and deposition (e.g. [11,12]). These studies have assisted data interpretation from the more complicated case of scaling of semi-permeable desalination membranes, that form spacer-filled narrow channels, in the commercial Spiral Wound Membrane (SWM) modules (e.g. [13–15]); however, significant knowledge gaps still exist, mostly related to the mechanism(s) of scale formation on membranes and to

* Corresponding author.
E-mail address: karabaj@cperi.certh.gr (A.J. Karabelas).

http://dx.doi.org/10.1016/j.desal.2017.04.009
Received 21 November 2016; Received in revised form 21 March 2017; Accepted 14 April 2017
Available online 09 May 2017
0011-9164/ © 2017 Elsevier B.V. All rights reserved.

the interaction of the scaling species with the membranes under the prevailing complicated flow conditions [16,17].

In a desalination plant comprised of a multitude of pressure vessels, each one usually containing 6 to 8 Spiral Wound Membrane (SWM) elements in series, the situation in respect of fouling-scaling is more complicated and apparently quite different than the aforementioned cases of "pure" scaling and organic fouling (e.g. [18,19]). For instance, in the common cases of brackish- and waste-water desalination, even with a small concentration of the ever-present organic foulants (e.g. [20]), there is a tendency for increased organic fouling in the leading SWM elements of pressure vessels, whereas the scaling potential of retentate tends to increase in the tail elements due to permeate withdrawal; moreover, it appears that in most cases, dissolved organic foulants are present in the retentate of *tail elements*, where supersaturation of inorganic salts develops. Therefore, this part of the desalination plant, where phenomena of *combined scaling-fouling* are very likely to take place, is of particular interest to this study. Reports on pilot studies with realistic feed-fluids and related membrane autopsies [20] tend to confirm the above picture in general, even though variations of fouling evolution and spatial profiles certainly depend on several other factors, notably including the feed-water origin and its degree and type of pretreatment (e.g. [19]).

Experimental studies on the abovementioned interaction of foulants with scale forming compounds on desalination membranes are rather limited; in most of them, scaling is studied on a *pre-formed* fouling layer. There are studies of calcium sulfate scaling on desalination membranes on which either a biofouling layer (e.g. [21,22]) or an organic layer (e.g. [23,24]) has been pre-formed. Most of these studies, performed with different protocols and significant bulk supersaturation, suggest that the pre-deposited fouling layers tend to enhance scaling. Hou et al. [21] reported that the amount of $CaSO_4$ and size of crystals deposited on a biofouled membrane was greater than that on non-fouled membrane; additionally, a denser and thicker bio-fouling layer exhibited reduced permeability, resulting in increased Ca^{2+} rejection. Experimental results of Thompson et al. [22] showed that flux decline, surface coverage and number concentration of mineral scale were greater in the presence of a pre-existing biofilm compared to a clean membrane. Furthermore, gypsum rosette-type crystals were observed within (and some protruding out of) the biofilm, which was attributed to enhancement of concentration polarization due the biofilm. Liu and Mi [23] ran scaling experiments with Forward Osmosis (FO) membranes, preconditioned by humic acids (HA), sodium alginates (SA) and protein (BSA), and fluid of initial supersartutation index reported to be 1.3 (S = 4.5). Their test results suggested a significant *scaling enhancement* effect by HA and SA, whereas BSA appeared to hinder gypsum crystal formation and to reduce flux decline due to scaling. Wang et al. [24] also pretreated nanofiltration (NF) membranes by solutions with dissolved HA, SA and BSA foulants, employing a different protocol; they reported greater scaling tendency of membranes pre-treated with HA and SA compared to BSA-treated and virgin membranes. On the contrary, Lee et al. [25] by mixing HA at small concentration (0.2 to 10 mg/L·HA) with feed solution, reported that a strong $CaSO_4$ *scale inhibition* effect was obtained in RO membrane desalination.

In efforts to gain insights into the complicated dynamic interaction between polysaccharides and the scale forming calcium ions, right at, and near, the semi-permeable polymeric membrane during desalination, it is rewarding to consult the significant body of literature regarding the following issues: a) the complexation of macro-molecular polysaccharides with calcium and b) the interaction of polysaccharides with the common polyamide RO-membrane active layer in the presence of Ca-ions. The complexation of Ca-cations with alginates (of interest here) leading to gel formation has been studied in depth in the field of bio-materials (e.g. [26,27]) and fairly well in the case of fluids, containing such species, that are treated for desalination [10]. It is well documented that Ca ions can readily substitute Na ions in SA solutions, forming stable regular macro-molecular structures (e.g. [28,29]) and agglomerates, which (through membrane filtration) tend to deposit as fairly coherent viscoelastic gel-type fouling layers [30]. Recent studies employing molecular dynamics simulations [31,32] offer valuable insights into the cross-linking of Ca ions through the *carboxylate groups* of mannuronic and guluronic acid (comprising the alginates) and corroborate the results of experimental studies (e.g. [33,34]) showing the strong binding/complexation of Ca with the alginate macro-molecules, through substitution of the weakly bound Na [31]. Similarly, results of experimental studies on the "calcium bridging" effect and the significant adhesion force between alginate gels and polyamide (PA) membrane surface [33] are corroborated by the molecular dynamics simulations [31,32]; the latter studies explore and quantify the ionic binding force developing by the Ca-mediated bridging between the PA chains and the alginate gel. Finally, a significant body of literature, most relevant to this study, deals with the *inhibition effect* of water soluble polymers on calcium salt precipitation. Indeed, it has been known for a long time (e.g. [35]) that polymeric compounds (carboxymethyl cellulose, CMC, poly-methyl acrylate, PMA, poly-acrylic acid, PAA) containing carboxylic groups (as the alginates) are quite effective as growth inhibitors of $CaSO_4{\cdot}2H_2O$. More recently, Lioliou et al. [36] by investigating the (PAA) as inhibitor of $CaSO_4$ precipitation (for concentration in the range 1 to 100 ppm), present results that are in line with the older studies. In summary, considering the results from all the above studies, it is uncertain whether the rather strong Ca-polymer (SA and PA) interactions and the Ca-alginate gel formation will tend to inhibit or enhance membrane scaling during RO/NF desalination.

In view of the above uncertainties and the insufficient information regarding scaling of desalination membranes from feed-waters containing polysaccharides, this study is focused on the effect of relatively small concentration of alginates (representative of conditions prevailing in desalination plants) on $CaSO_4$ deposition/scaling during desalination. The employed rather small supersaturation ratio (S ~ 1.4) of the synthetic feed solution is considered typical of conditions prevailing at the tail elements of brackish- and waste-water desalination plants. The experiments are carried out in a set-up involving desalination cells operating under constant pressure and agitation. The initial stages of $CaSO_4$ membrane scaling are studied in efforts to clarify the main effects of organic foulants on scaling.

2. Theoretical background

The *supersaturation ratio S*, and the saturation index SI, of calcium sulfate solution are expressed as follows [37,38]:

$$S = \left[\frac{IAP}{K_a}\right]^{1/2} \tag{1a}$$

$$SI = 2{\cdot}\log S \tag{1b}$$

where IAP is the calcium and sulfate ions activity product ($a_{Ca^{2+}} \cdot a_{SO_4}{}^{2-}$) and K_a is the solubility product. IAP and K_a are obtained by employing the PHREEQC code (version 2.18.00) [39] using the "Pitzer" database. The PHREEQC computer program is based on a thermodynamic ion-association model implementing the extension of the Debye-Hückel theory.

The tests on desalination membrane fouling/scaling were conducted in cylindrical dead-end filtration cells with agitation, as subsequently described in detail. Due to the concentration polarization effects, the concentration of calcium and sulfate ions at the surface of a clean membrane is greater than in the bulk solution and is commonly estimated, for complete salt rejection, as follows [40]:

$$[C_w/\ C_b] = \exp\,(J/k_m) \tag{2}$$

here Cb and J are the known bulk species concentration and permeate flux, respectively, and k_m (m/s) the mass transfer coefficient at the membrane surface. The latter can be obtained from a reliable correla-

tion derived from experiments [41] conducted in the same desalination pressure cells used in this study:

$$Sh = 0.49 \cdot \mathrm{Re}^{0.55} \cdot Sc^{0.33} \quad (3)$$

where Sh is the Sherwood number ($Sh = k_m \cdot r/D$), the characteristic length r, for the case of stirred cell, is the radius of active membrane specimen surface, D the diffusion coefficient of ionic species, Sc the Schmidt number ($Sc = \frac{\nu}{D}$) and ν the liquid kinematic viscosity. The Reynolds number is given as $\mathrm{Re} = \frac{\omega \cdot r^2}{\nu}$, where ω is the stirrer angular velocity (rad/s). The diffusion coefficient of main ionic species was obtained according to [42] and the values are given in the supplement (S6) together with information on kinematic viscosity calculation.

The concentration C_w is used for estimating the supersaturation ratio at the membrane surface, S_w, which in these tests was 5%–10% greater than the value determined for the bulk solution, depending on experimental conditions.

3. Materials and methods

3.1. Chemical reagents and analytical methods

Calcium sulfate, dealt with in this study, is frequently detected on scaled desalination membranes, as calcium sulfate dihydrate ($CaSO_4 \cdot 2H_2O$), commonly known as gypsum [13,14]. In all the present tests, the synthetic solutions employed were characterized by (the same) nearly constant gypsum bulk supersaturation ratio S ≈ 1.4, to facilitate comparisons. This level of supersaturation S is likely to prevail at the tail SWM elements in RO pressure vessels due to the retention of calcium and sulfate ions [43].

Sodium alginate, selected as model organic foulant, has a molecular weight distribution in the range 12 to 80 kDa. More details regarding alginate characteristics can be found elsewhere [30,44]. All solutions were prepared by dissolving the analytical grade chemicals, obtained from Sigma-Aldrich, in deionized (Milli-Q) water. A stock solution of sodium alginate (1000 mg/L) was prepared by dissolving a predetermined amount of alginate powder in deionized water, under continuous stirring, at room temperature for 24 h. The stock solution was kept at 4 °C.

The feed solutions were well characterized, prior to filtration tests, by measuring pH and conductivity via a laboratory multi-parameter meter (inoLab 750 pH/ION/Cond multilab, WTW, Germany); turbidity was measured by a portable turbidimeter (HF Scientific Inc., DRT-15 CE, USA). Measurements, including concentration of total dissolved solids (TDS), calcium, sulfate and chlorine ion concentration were also performed [45]. The Na^+ concentration was determined stoichiometrically.

The detailed physicochemical characteristics of feed solutions, other experimental conditions and key parameter values of the various tests performed in this study, are all listed for convenience in Table A1 (Appendix). In this table, test numbers appear in the top row; the second row (in parentheses) indicates the companion test ran simultaneously in the second pressure cell, under the same conditions, but with a different fluid composition for comparison.

3.2. Experimental set-up

Experiments to investigate the interaction between organic fouling and mineral scaling on desalination membranes were conducted, in dead-end filtration mode with agitation, using an experimental set-up, comprising a pair of high pressure thermostated stirred cells, as shown in Fig. 1. The operation of the cells is described in detail elsewhere [46,47].

To collect data systematically and facilitate comparisons, two cells were operated simultaneously under identical experimental conditions, but with different feed solution compositions. The effective membrane area in each cell was 9.1 cm^2. High pressure nitrogen was used to maintain constant the applied pressure, in the range 150 to 170 psi (~1000 to ~1200 kPa). In the stirred test cell, containing the synthetic feed solution, deionized water was continuously supplied from a second pressure vessel to compensate for the permeate removal; thus, the chemical composition of the feed water inside the test cell (including the supersaturation ratio and the osmotic pressure) remained essentially *constant* during the desalination period, irrespective of the permeate withdrawal, which was generally small. The temperature was maintained at 25 °C, through a constant temperature bath. The experiments were performed under a constant stirring rate of 250 rpm; this stirring rate was selected because it has been shown [41] that it leads to a space-average shear stress at the membrane surface roughly equal to that prevailing in spacer-filled channels of SWM modules at usual cross-flow velocity ~ 15 cm/s. The permeate flux was determined by measuring the permeate mass through electronic balances (PL602-S Mettler-Toledo AG, Switzerland) connected to a computer for data acquisition.

A low-pressure reverse osmosis, thin film composite polyamide membrane (CPA2, Hydranautics, USA), was employed in this study. Membrane coupons in appropriate dimensions were cut from a commercial SWM element. After rinsing with deionized water, the coupons were stored in an aqueous solution of 0.75% $Na_2S_2O_5$ (sodium meta-bisulfite) and kept in a refrigerator at 4–5 °C. Furthermore, mixed cellulose ester membrane filters (ME 24/21 ST, Whatman GmbH, Germany), of nominal pore size ~0.20 μm, were used for filtration of feed and retentate solutions, to retain $CaSO_4$ for analysis.

3.3. Experimental procedures

After the membrane preparation and compaction [46,47], the pressurized auxiliary vessel was filled with approx. 700 mL Milli-Q water whereas the pressure test-cells were filled completely with approx. 300 mL synthetic feed water; the latter was fully characterized regarding physicochemical properties. It should be pointed out that the free air volume above the aqueous solution was eliminated by totally filling the cell. The experiments started within the first 10 min after the solution preparation. A description follows of the three types of tests performed in this study.

3.3.1. Scaling tests

The synthetic solution of inorganic scale-forming species consisted of Ca^{2+} and SO_4^{2-} ions at equimolar concentrations of ~35 mM; it was prepared by rapidly mixing equal quantities of aqueous $CaCl_2 \cdot 2H_2O$ and Na_2SO_4 solutions in deionized water.

3.3.2. Combined fouling/scaling tests

The initial solution comprised Ca^{2+} and SO_4^{2-} at equimolar concentrations of 35 mM with the addition of Sodium Alginate (SA). The feed water, with SA concentration either 2 mg/L or 10 mg/L, was prepared as follows. Sodium alginate stock solution was diluted to the desirable concentration with deionized water and an appropriate quantity of anhydrous sodium sulfate (Na_2SO_4) was added to it. An equivalent solution of calcium chloride ($CaCl_2 \cdot 2H_2O$) was also prepared. The final feed water solution was prepared by slowly adding the $CaCl_2 \cdot 2H_2O$ solution to the sodium alginate and sodium sulfate solution under continuous agitation. In the tests, the synthetic solution of combined foulant/scalant was filtered through the desalination membrane in the dead-end cell under constant pressure for various time periods; i.e., 90, 120 and 240 min. The deposits on the membrane and

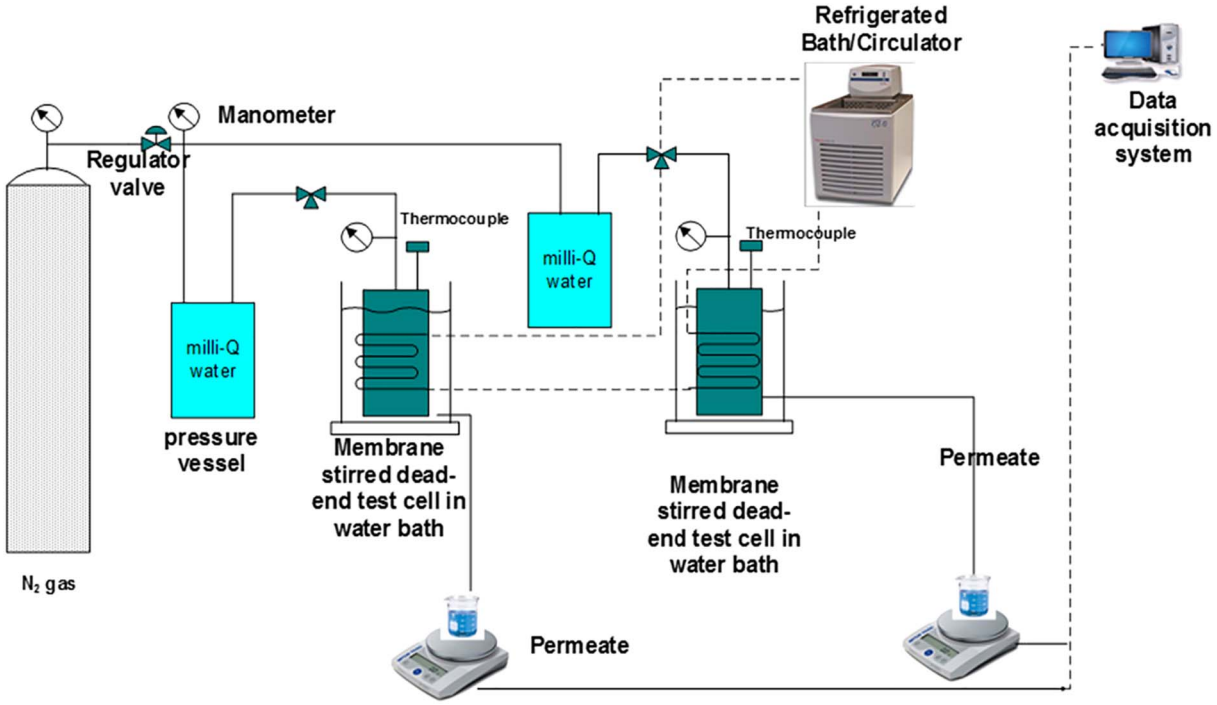

Fig. 1. Experimental set-up, involving pressurized dead-end filtration cells, for studying membrane scaling and fouling.

the solids/precipitate of the retentate were analyzed at the end of tests. In each such test, aiming to investigate the effect of organic foulants on $CaSO_4$ crystallization, a scaling test (with no SA addition) was performed in parallel, under identical conditions, for comparison.

3.3.3. Scaling tests after fouling tests

These experiments were conducted in order to investigate the effect of a *preformed* organic fouling layer on the incipient scaling/crystallization of $CaSO_4$ on the membrane. Two separate solutions were prepared; i.e. a solution of organic foulant and another with the inorganic scale-forming species. In the former solution, the sodium alginate and calcium ion concentrations were 2 or 10 mg/L and 2 mM, respectively. A solution of sodium alginate was prepared by diluting the stock solution to the desirable concentration with deionized water. A Ca^{2+} solution was prepared by diluting the appropriate quantity of calcium chloride dihydrate in deionized water. These two solutions were rapidly mixed under agitation. In two cases the ionic strength of the foulant solution was increased with the addition of Na_2SO_4 in the SA solution. The test solution was prepared by rapidly mixing equivalent quantities of sodium sulfate and calcium chloride solutions. The organic foulant solution was filtered through the desalination membrane for 100–120 min under constant pressure and agitation at 250 rpm. After the end of this test, the pressure cell was emptied, filled with scale-forming solution, and filtered under constant pressure, as in the preceding case (3.3.1) with clean membrane.

3.4. Treatment of specimens – Data collection

The disk-type membrane coupons, after the termination of dead-end tests, were left to dry under ambient conditions. Three small pieces (5 mm × 5 mm) were cut from each membrane disc, from the region near the specimen periphery, the disc center, and the area between them ("middle"), for SEM examination. Specimens were gold sputtered and analyzed by employing scanning electron microscopy (SEM, JSM-6300 Scanning Electron Microscope, JEOL Ltd., Japan) [47]. As outlined in previous work [17], typical *Secondary Electron Images* (SEI) as well as *Backscattered Electron Images* (BSI) were obtained, in order to enhance contrast and acquire more detailed information on the membrane scale formation. Qualitative chemical characterization of the precipitates on the membrane surface was obtained by the X-ray spectrometer unit (EDS, LINK ISIS, Oxford Instruments, UK) connected to the SEM system.

The deposited scale on the membrane was determined through dissolution; i.e. the remaining specimen from a scaling test, was immersed in a known volume of HCl solution, prepared by diluting 5 mL of concentrated HCl in 1 L of deionized water. The deposits on the membrane coupons obtained from combined fouling/scaling tests were treated differently; they were first immersed in a KOH (200 mM) solution and subsequently in HCl solution. Each dissolution step was conducted under agitation for at least 12 h. Calcium was determined in an Inductively Coupled Plasma unit (Optical Emission Spectrometer, Model Optima 4300 Dv, PerkinElmer, USA). From this Ca measurement, the mass of the corresponding deposited solids (considered to be gypsum) was calculated stoichiometrically for all cases, to facilitate data comparison. It should be noted that the validity of the assumption made here (i.e. that *all Ca* is bound to gypsum) is impossible to assess in the case of tests with SA, where Ca ions can be trapped in the fouling layer and/or complexed in the alginate gel [10]; however, it is considered (for reasons discussed below) that the respective error does not impact on the basic trend of the data.

Additionally, feedwater samples taken at different time intervals after the preparation, and the retentate solutions from the desalination tests were filtered through a 0.20 μm mixed cellulose ester membrane to separate precipitated $CaSO_4$ and foulants. These filters were also prepared for SEM observations in order to determine the characteristics of retained solids and foulants existing in these bulk solutions. The residue retained by the filters was also dissolved, employing the aforementioned protocol, for calcium determination.

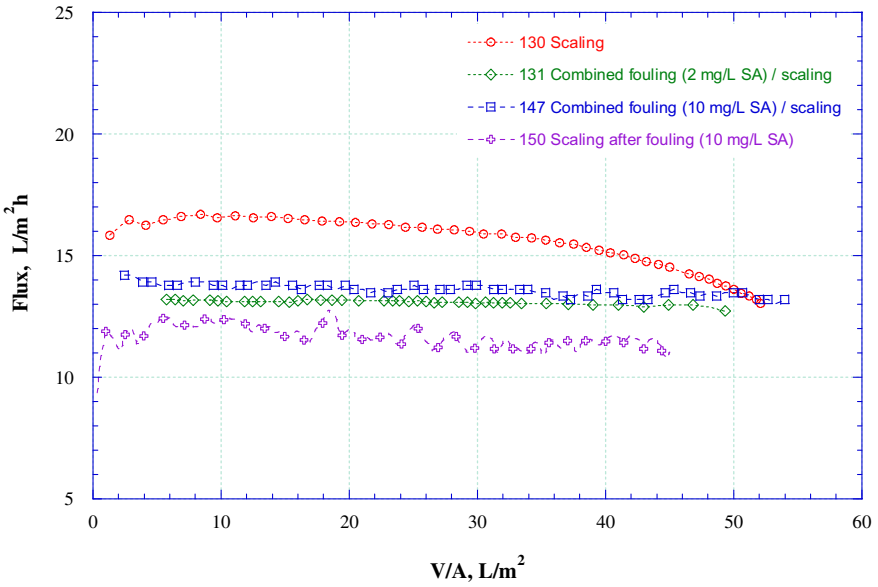

Fig. 2. Flux variation of typical scaling test, combined fouling/scaling tests, and consecutive fouling/scaling test, versus specific permeate volume.

4. Results and discussion

4.1. Overview of experimental conditions and key process parameters

Table A1 summarizes the experimental conditions and key process parameters determined in 23 successful experiments. In all scaling tests the Ca^{2+} concentration was within the narrow range 32.63 to 34.81 mM, and the pH of the feed solutions in all cases was within 5.6 to 6.2 with no adjustment. The feed solution conductivity in almost all scaling tests (with or without alginates) was within the range 10.500 to 11.300 μS/cm. Consequently, depending on other small solution differences, the bulk supersaturation ratio S was in all cases within the narrow range S = 1.36 to 1.48, with a concomitant supersaturation ratio at clean membrane wall estimated to be S_w = 1.45 to 1.55. The constant applied pressure was ΔP_{ap} = 170 psi (1172 kPa) in almost all cases. Although there was some variability, the initial permeate flux was at the level of ~14 L/m^2 h, which is considered typical of fluxes prevailing at the tail SWM elements where retentate supersaturation appears, particularly in *brackish-water* desalination plants prone to scaling [43]. Under these conditions, in almost all cases, the measured salt rejection was within the range 97.2% to 98.6%, with no detectable systematic effect of particular experimental conditions.

In Fig. 2 typical flux profiles from the present tests are included. In the case of membrane *scaling experiments* in the absence of alginates, the flux initially tends to be practically unaffected by depositing $CaSO_4$. Only when the membrane-surface coverage becomes significant, the flux tends to gradually decline by following a *convex* curve, as has been observed in other similar studies [22,48]; this flux reduction trend is due to the localized, particulate type, of scale-deposits that grow on the membrane in all three dimensions and only gradually block membrane pores as their number increases. However, a different, *concave* flux reduction curve, is commonly observed in biofouling and organic fouling studies (e.g. [22,49]); this is due to the tendency of organic macromolecules and agglomerates to spread laterally on the membrane, thus forming rather rapidly a layer, blocking pores and causing flux reduction right after the start of filtration.

In the case of combined fouling – scaling, with the *higher SA concentration (10 mg/L)*, there is a modest initial decline due to alginate deposition. Beyond this initial period, lasting approx. 60 min, the flux remains practically stable, indicating no substantial increase of fouling resistance to permeation thereafter. Considering the conditions of present tests (i.e. constant agitation and wall shear forces, rather high Ca concentration) one may attribute this flux stabilization to existence of loose alginate agglomerates that tend to deposit on the already fouled membrane, but cannot lead to a coherent layer (beyond an initial thickness) as they may be detached by flow shear. The SEM pictures of membrane surface, shown in Figs. S4 and S5 (10 ppm·SA) (Supplement), tend to support this hypothesis; indeed, judging by the presence of distributed (at small scale) darker patches on the membrane surface, the alginate deposits seem to be of non-uniform thickness, likely due to deposition of agglomerates. For the combined fouling-scaling tests at *small SA concentration (2 mg/L)*, the flux appears to attain at short time a nearly constant value (Fig. 2). For this case, the evidence of alginate agglomerates (distributed unevenly on the membrane) is much more clear, as shown in Fig. S2 and S3 (2 ppm·SA) in the Supplement and further discussed in the following. Therefore, the above-mentioned hypothesis of nearly stable fouling layer, determined by the shear field, may hold in this case as well. It should be noted at this point that Mo et al. [50] have shown experimentally that, above a certain Ca concentration, alginate agglomerates develop in the balk and that NF membrane fouling tends to be retarded. Regarding the tests of *scaling after a fouling layer was deposited on the membrane*, the flux did not show significant reduction (Fig. 2); it will be recalled that in the present scaling tests [at rather small supersaturation index SI ~ 0.3], relatively thin fouling layers were pre-formed through filtration of dilute alginate solutions. However, it has been reported [23] that in similar experiments using FO membranes, with thicker preformed layers (using feed SA concentration 200 mg/L) and greater supersaturation (SI = 1.3), compared to the present study, very significant flux reduction was obtained during scaling.

4.2. Scanning electron microscopy study

4.2.1. Scaling – No alginates present

As shown in Fig. 3a,b, in the absence of alginates, significant $CaSO_4$ deposition occurred on the membrane, with extensive surface coverage, which is in line with the measured flux reduction (Fig. 2). In the absence of polysaccharide, the crystal habit of the developed and/or

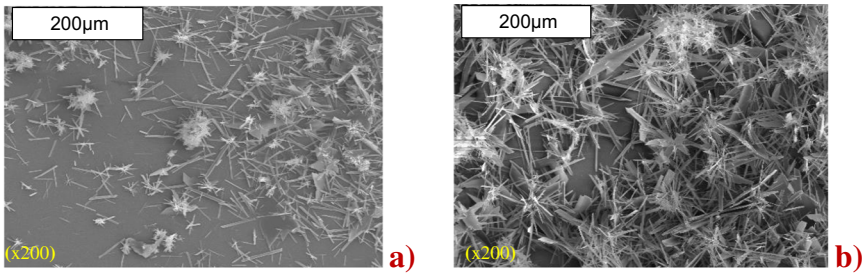

Fig. 3. SEM images from *scaling tests*: a), b) $CaSO_4$ crystals deposited/developed on the desalination membrane. c), d) $CaSO_4$ crystals filtered out of the retentate. e), f) $CaSO_4$ particles filtered out of the stagnant feed solution.

deposited $CaSO_4$ is that of well-known elongated gypsum crystals, which is the result of uninhibited and rapid growth of the [111] faces (e.g. [51]). The pictures in Fig. 3, allow an enlightening qualitative comparison of the mass density of $CaSO_4$ crystals on the membrane (Fig. 3a,b) with the concentrations of $CaSO_4$ crystals in the retentate (after the end of experiments- Fig. 3c,d) and in the stagnant feed solution batch (Fig. 3e,f), which were obtained after filtering out the dispersed solids by a 0.20 μm filter. The following observations are made: a) The very significant $CaSO_4$ surface density on the membrane and the larger size of crystals (Fig. 3a,b), compared to those in the agitated bulk (Fig. 3c,d), clearly suggest that the mechanism of crystal-particle growth *right at the surface* is important (as also discussed elsewhere [16,17] even though nucleation in the solution bulk, and deposition of crystallites from the bulk, can also contribute to membrane scale formation. b) The smaller concentration of precipitated $CaSO_4$ crystals in the stagnant feed solution (Fig. 3e,f), compared to the agitated retentate (Fig. 3c,d), is a manifestation of the positive effect of convective mass transfer to crystal growth rate in the latter case. Moreover, the smaller and more uniform size of developing crystals in the agitated retentate, compared to stagnant feed-solution (containing many elongated crystals - Fig. 3f), is attributed to agitation/mixing and the possible needle breakage in the former case. It should be added that quantitative information regarding the aforementioned solids surface density on the membrane and $CaSO_4$ crystal concentration in retentate and feed solutions is presented in Tables S1 and S2 of Supplement.

It should be pointed out that marks (S) and (B) made in SEM pictures of this paper designate "*secondary electron*" and "backscattered electron" mode of imaging (Section 3.4). If not otherwise designated, images correspond to the common "*secondary electron*" mode.

4.2.2. *Combined fouling-scaling*

Results from tests with the smallest SA concentration (i.e. 2 mg/L) reveal a drastic inhibitory effect of SA polysaccharides on $CaSO_4$ crystallization. Indeed, in two of the tests (No 128 and 131, Table A1) the observed crystals are very limited, compared to the preceding case of scaling with no SA present; this is also quantified through the

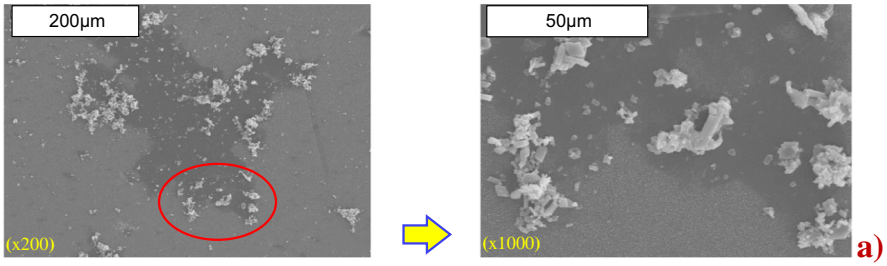

Membrane fouling-scaling a) Test No 131 (240 min); permeatevolume 47.6 mL.

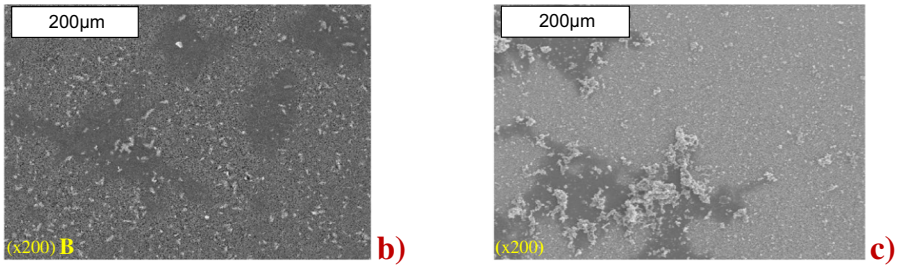

Combined fouling-scaling tests – Retentate

b) 120 min after preparation of feed solution; filtration of 250mL (Test No 128, 90 min)

c) 265 min after preparation of feed solution; filtration of 100mL (Test No 131, 240 min)

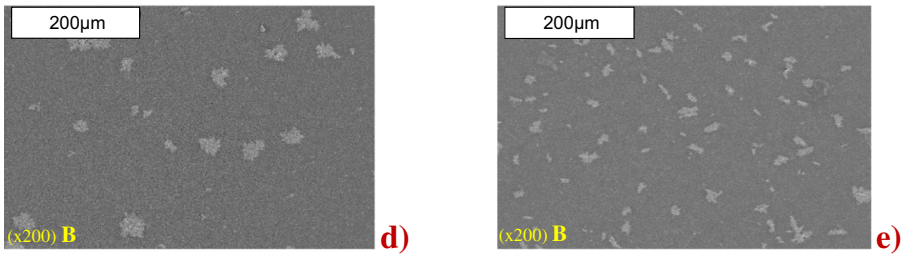

Combined fouling-scaling test - Feed solution

d) ~10 min after preparation of feed solution; filtration of 100mL (Test No 131, 2 mg/L SA)

e) 240 min after preparation of feed solution; filtration of 100mL (Test No 131, 2 mg/L SA)

Fig. 4. SEM images from *combined fouling-scaling*, 2 mg/L·SA. a) $CaSO_4$ crystals on alginate deposit and membrane. b), c) $CaSO_4$ crystals and alginate agglomerate filtered out of the retentate. d), e) $CaSO_4$ particles filtered out of the feed solution.

dissolution measurements presented in subsequent section. In two other similar tests (No 133, 148, Table A1) the scale deposits cannot be clearly identified (Figs. S2 and S3, Supplement). The SEM pictures from tests no 128 and 131 included in Fig. 4 show the significant effect of polysaccharides on $CaSO_4$ crystallization even at small SA concentration (i.e. 2 mg/L). Upon inspection of these pictures the following observations can be made:

a) The development of $CaSO_4$ crystals appears to occur preferentially on patches deposited on the membrane (dark areas in Fig. 4a), likely comprising alginate gels. One may hypothesize that the alginate gel matrix (with the relatively high calcium concentration - complexed and in free ionic form) favors $CaSO_4$ nucleation; the fact that such agglomerates, loaded with $CaSO_4$ crystals, also exist in the retentate (Fig. 4c) seems to support this hypothesis. However, one cannot exclude the possibility that these alginate agglomerates, formed right after mixing of feed solution, also act as a kind of coagulant for loose nuclei and crystallites created in the solution bulk.

b) The alginates apparently act as $CaSO_4$ *crystal growth inhibitor*. It is, indeed, well documented in the literature (e.g. [35,36,52]) that very small quantities of water-soluble polymers (especially those containing carboxylic groups, as the alginates) act as retarders of $CaSO_4$ crystal growth. As the pictures in Fig. 4a,c clearly show, the habit of the $CaSO_4$ crystals is significantly affected by the polysaccharide; specifically, instead of the uninhibited, elongated gypsum crystals (Fig. 3a,b), some prismatic shapes dominate that tend to agglomerate. Interestingly, a quite similar crystal habit was obtained by Lioliou et al. [36] in tests with Polyacrylamide (PAA) inhibitors of $CaSO_4$ crystal growth. Finally, it should be stressed that in the other two similar tests (No 133, 148, Table A1) with 2 mg/L SA, the inhibition effect was even stronger, with barely identifiable $CaSO_4$ crystals.

c) The very small concentration of seemingly amorphous $CaSO_4$ tiny particles, separated from the stagnant feed solution batch (Fig. 4d, e), provides additional evidence regarding the inhibition action of the alginates.

Fig. 5 includes SEM pictures related to the effect of alginates, at the higher tested concentration (10 mg/L), in the supersaturated $CaSO_4$ solution. The main observations here are as follows: a) The effect of alginate on incipient $CaSO_4$ crystallization *on the membrane* is more pronounced in this case. Very small (of order 10 to 100 μm in diameter) *amorphous $CaSO_4$ platelets*, appear to be rather uniformly distributed

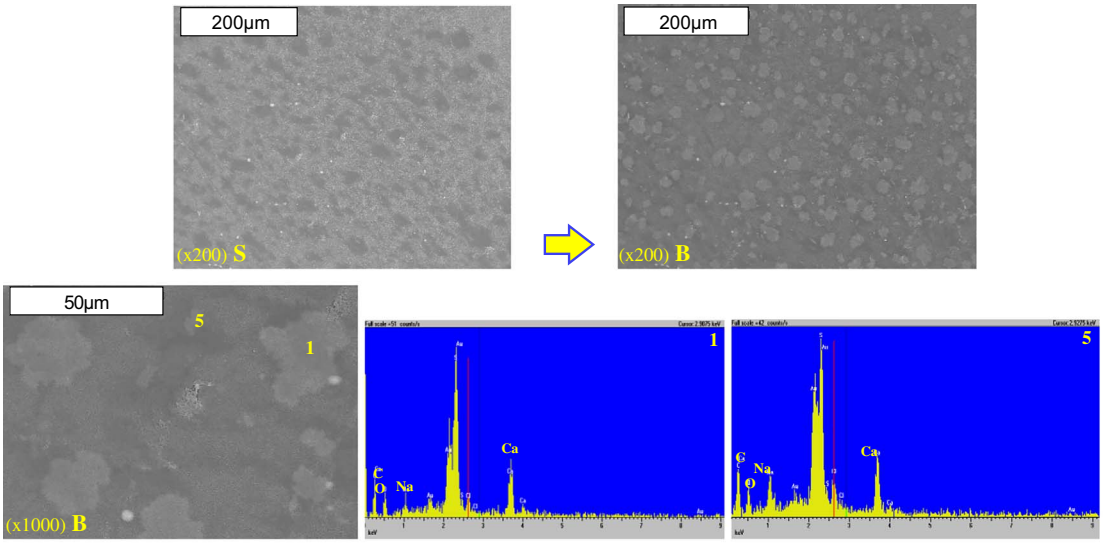

Membrane fouling-scaling a) Test No 129 (240 min); filtration of 51.2 mL; EDS analyses points #1, #5.

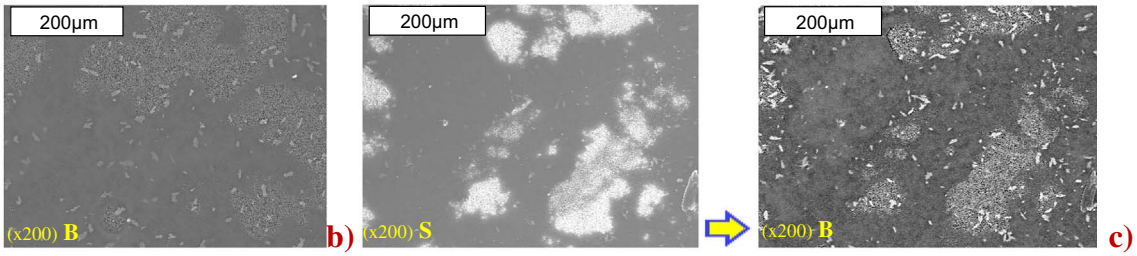

Combined scaling- fouling test – Retentate

b) 260 min after preparation of feed solution; filtration of 100 mL (Test No 129, 240 min)

c) 250 min after preparation of feed solution; filtration of 100 mL (Test No 137, 240 min)

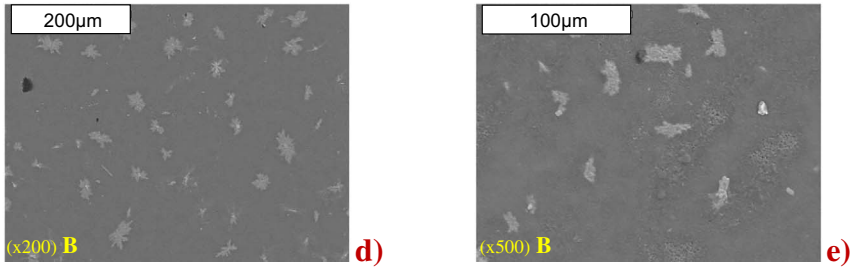

Combined fouling-scaling test – Feed solution

d) ~5 min after preparation of feed solution; filtration of 100 mL (Test No 129, 10mg/L SA)

e) 240 min after preparation of feed solution; filtration of 100 mL (Test No 129, 10mg/L SA)

Fig. 5. SEM images from *combined fouling-scaling*, 10 mg/L·SA. a) $CaSO_4$ particles developed within alginate fouling layer. b), c) $CaSO_4$ particles and alginate agglomerate filtered out of the retentate. d), e) $CaSO_4$ particles filtered out of the feed solution.

inside the alginate fouling layer covering the membrane surface (Fig. 5a); this is confirmed by the Energy-dispersive X-ray spectroscopy (EDS) qualitative analysis at specific locations on the membrane. It should be noted that RO SWM module autopsies by Tran et al. [18] also show particulate matter embedded in an amorphous organic fouling layer, likely comprising polysaccharides. The mass of those tiny $CaSO_4$ platelets is small, as also estimated from dissolution tests and reported below. No well-formed crystals, of typical elongated or prismatic shape, were identified. Therefore, this mode of seemingly very slow development of solid phase, under the present conditions and SA concentration, clearly suggests that the alginates act as an effective inhibitor of $CaSO_4$ crystallization. b) The tiny particles detected in the *retentate* (Fig. 5b,c), which appear to be attached to alginate-gel, confirm the strong inhibitory action under these conditions. Similarly, tiny amorphous particles are detected (Fig. 5b,c), through filtration of *stagnant feed* solution. However, the rather small difference between particles corresponding to ~5 min (i.e. at solution preparation) and 240 min (Fig. 5d and e), may suggest that these particles, once created during initial solution mixing, tend to grow at a very small rate; these observations are also corroborated by the dissolution test results,

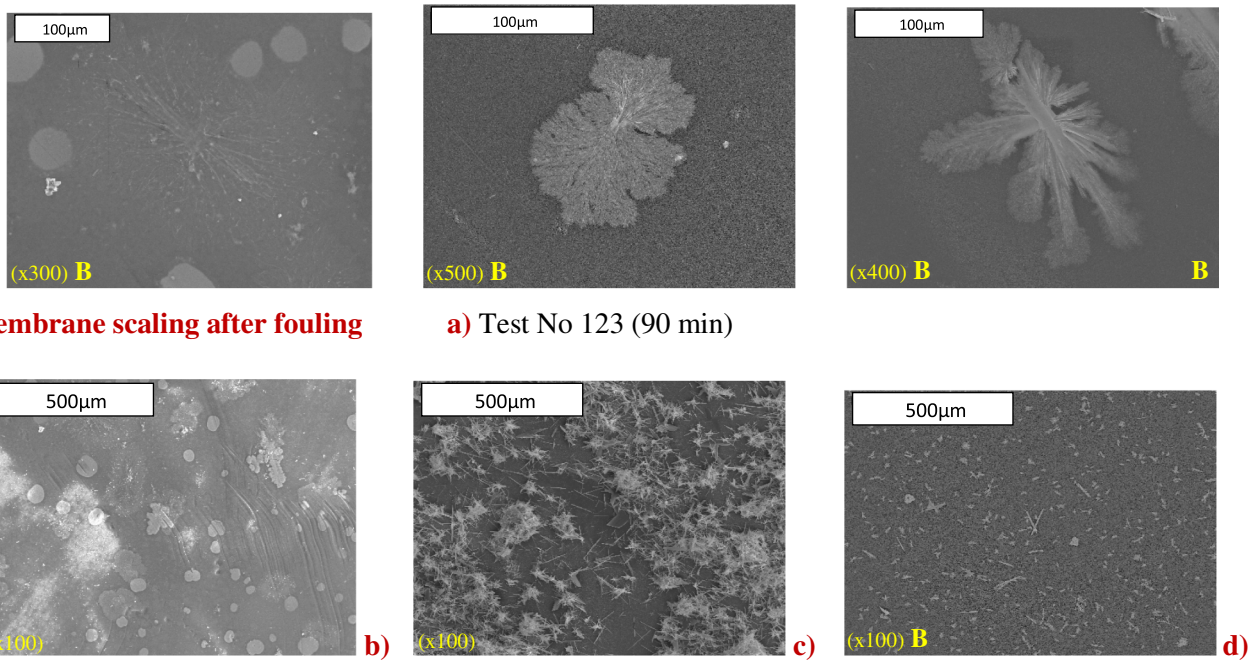

Fig. 6. SEM images from *scaling after membrane fouling*. a), b) Membrane scaling; Test No 123 (90 min). c) Membrane scaling; Test No 142 (240 min, 2 mg/L SA + 2 mM Ca^{2+} + + 35 mM Na_2SO_4). d) Retentate; Test No 123 (120 min after feed preparation; filtration of 250 mL).

subsequently presented. It should be noted that the two SEM images from retentate filtration in Fig. 5c, showing tiny particles have been obtained with different contrast. c) Considering the above evidence, *threshold inhibition* [53] is likely the prevailing mechanism in this case (as opposed to crystal growth retardation); i.e., the alginate macromolecules tend to block the development of supercritical nuclei.

4.2.3. Scaling after membrane fouling

Fig. 6 includes SEM pictures regarding the case of membrane scaling after depositing a fouling layer. It is clearly shown in Fig. 6a, b (from test no 123; fouling by solution with 10 mg/L SA) that some qualitative similarities exist between this case and the one of combined scaling-fouling; indeed, some amorphous disc-like $CaSO_4$ tiny particles appear to have grown inside the alginate gel deposit. However, some relatively large $CaSO_4$ crystals also develop into and perhaps out of the fouling layer; these two-dimensional *rosette-type* crystalline particles are similar to the ones presented by [22] in the same type of tests but under different conditions. It will be noted that the pictures in Fig. 6a,b correspond to a relatively short-time test (90 min); it is, therefore, expected that these $CaSO_4$ rosettes will tend to significantly grow with time and cover a larger portion of membrane surface, as observed in previous studies [14,22].

The picture in Fig. 6c shows significant crystalline deposits from a different test (No 142) ran at longer time (240 min); the fouling solution in this case contained only 2 mg/L SA, and was of greater ionic strength compared to the previous test (No 123, Fig. 6a,b). By comparison with Fig. 6a,b it appears that in this case (Test No 142) the effect of pre-deposited alginate layer is of much lesser significance, and the crystal habit resembles that of membrane scaling with no alginate pretreatment of membrane (Fig. 3a,b). However, to assess whether the pre-deposited fouling layer has an effect on the rate of deposition, determination of calcium and of deposited solids on the membrane is required, which is presented below. Regarding $CaSO_4$ precipitation in the retentate (Fig. 6d), it is interesting that it is quite small (with tiny particles of different shape) compared to the membrane deposits (Fig. 6a and b), which strongly supports the suggestion that mechanisms occurring at the membrane surface tend to dominate the scaling process during desalination [9,34].

It is of interest to note that in the fouling tests for treating the membrane, prior to scaling experiments (Test Nos 139–141, 143; Supplement Figs S6-S9), there was evidence of non-uniform fouling layers developing on the membrane; indeed, patches of different shade are identified on the membrane specimens, attributed to different mass of deposited foulants. It is hypothesized that, due to the significant calcium ion concentration, complexation with alginate molecules leads to agglomerates, possibly formed also in the bulk. The latter may be distributed non-uniformly on the membrane surface, likely influenced by the spatially variable flow pattern and wall shear stresses; Fig. S7 and S9 (Supplement) provides evidence of such effects due to the variable angular velocity components and the flow stagnation point at the centre of the disc-type membrane coupon.

4.3. Analytical determination of deposits on membranes and of precipitates in the bulk

The data included in this section (listed in Tables S1 and S2, Supplement) were obtained by dissolution of solids, deposited on the desalination membrane and on 0.20 μm filters, the latter from filtration of the retentate and the stagnant feed-solution batch; dissolution was followed by analytical determination of calcium, as described in preceding Section 3. From these analyses, key parameters were estimated such as the solids/gypsum mass density on the membrane surface (in mg/m^2) as well as the precipitate concentration (in mg/L) in the retentate and feed-solution bulk. In these estimates, the assumption was made that all the measured calcium was in the form of calcium sulfate dihydrate (gypsum). However, it is possible that a very small amount of calcium (estimated to be of order much less than 10 mg/m^2) could be adsorbed directly on the membrane and/or included (or

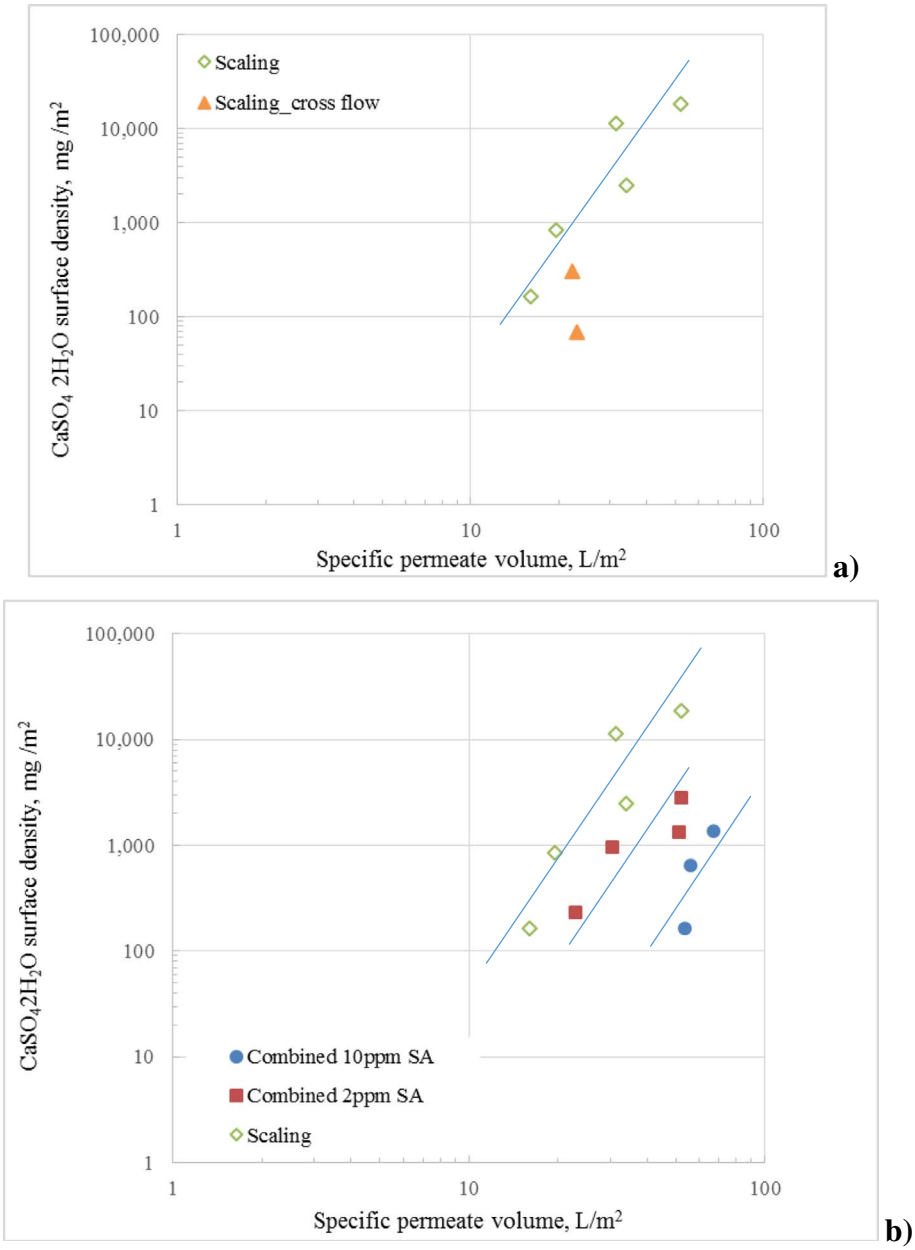

Fig. 7. *Scaling and combined fouling/scaling tests*. Equivalent gypsum deposit density on the RO membrane [mg/m^2], corresponding to measured calcium, versus the specific permeate volume from dead-end desalination experiments. a) Membrane scaling data in the absence of alginates. b) Scaling data in the presence of alginates; comparison with scaling data of case a).

complexed) in alginate mass retained on the filter; therefore, this experimental error is expected to lead to a small over-estimation of crystallized or precipitated solids.

In Fig. 7a the estimated surface density of gypsum, deposited on the membrane, is plotted versus the corresponding specific permeate volume (in L per m^2 of membrane surface area), for various tests in the absence of alginates (scaling tests). This type of data presentation is permissible because in all these tests, regarding the initial period of scaling, the bulk supersaturation ratio S is nearly constant (approx. 1.4). Moreover, the specific permeate volume is the most appropriate quantity to present such data for two reasons: First, differences due to flux and to experimentation time are accounted for; second, data presented in this manner have a greater archival value as they can be compared with results from other similar tests to investigate the effect of system parameters. The data of Fig. 7a are indicative of the fairly large rate of scaling of the desalination membrane even at this relatively small initial supersaturation ratio S ~ 1.4. A line has been drawn to indicate the data trend; the scatter is attributed to experimental error from various sources, including supersaturation ratio, flux, and clean membrane permeability variations [46]. In Fig. 7a two data points are also plotted from tests carried out in a similar study [17], employing a more realistic cross-flow test section (Fig. 12b, [17]); these points correspond to similar mean fluxes and supersaturation S. It is interesting that there is fair agreement with the present data, which supports the appropriateness of using the desalination pressure-cell under agitation to obtain data applicable to desalination in spacer-filled channels [41].

In Fig. 7b, $CaSO_4$ deposition data are plotted for the cases of

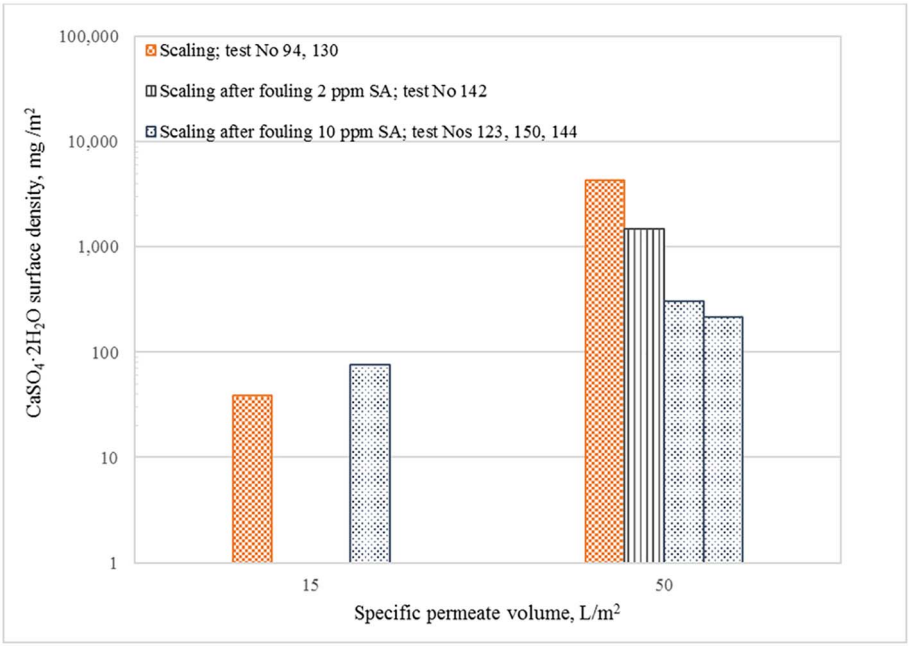

Fig. 8. *Scaling and scaling-after-fouling tests*. Equivalent gypsum deposit density on the RO membrane [mg/m^2], corresponding to measured calcium, at specific permeate volume ~15 and ~50 L/m^2 from dead-end desalination experiments.

combined fouling-scaling, in comparison to membrane scaling in absence of alginates. These data are in full accord with the qualitative conclusions drawn, in the preceding Section 4.2, on the basis of SEM pictures from the same cases. It is, therefore, quantitatively established that the presence of alginates in quite small concentration (2 mg/L SA), in a $CaSO_4$-supersaturated solution, inhibits growth of gypsum crystallites on the membrane; it is also noted that, despite the gypsum growth-retardation, the deposited solids mass on the membrane tends to significantly increase with time. In the case of greater SA concentration in solution (i.e. 10 mg/L), the drastic inhibition of $CaSO_4$ crystallization, indicated in the respective SEM pictures (Fig. 5), is quantitatively confirmed and clearly reflected in the deposition values plotted in Fig. 7b. Indeed, as shown in this figure, the solids mass surface density on the membrane in the presence of 10 mg/L·SA is more than an order of magnitude smaller than that of the alginate free solution, for the same fluid desalination period.

Fig. 8, depicts data (at two specific permeate volumes) on scaling after a membrane treatment with alginates of concentration 2 mg/L and 10 mg/L SA, in comparison with scaling of a clean membrane (no SA pre-deposited). As also concluded from observations of the SEM pictures, in the initial period of scaling dealt with here, the data for a specific permeate volume ~ 50 L/m^2 (~4 h filtration time) show that the pre-treatment of the membrane with a dilute polysaccharide solution, for a relatively short period of time, tends to inhibit $CaSO_4$ crystal development. Moreover, the smaller concentration of SA (2 mg/L, test 142) in the fouling/treatment solution (leading to less organic

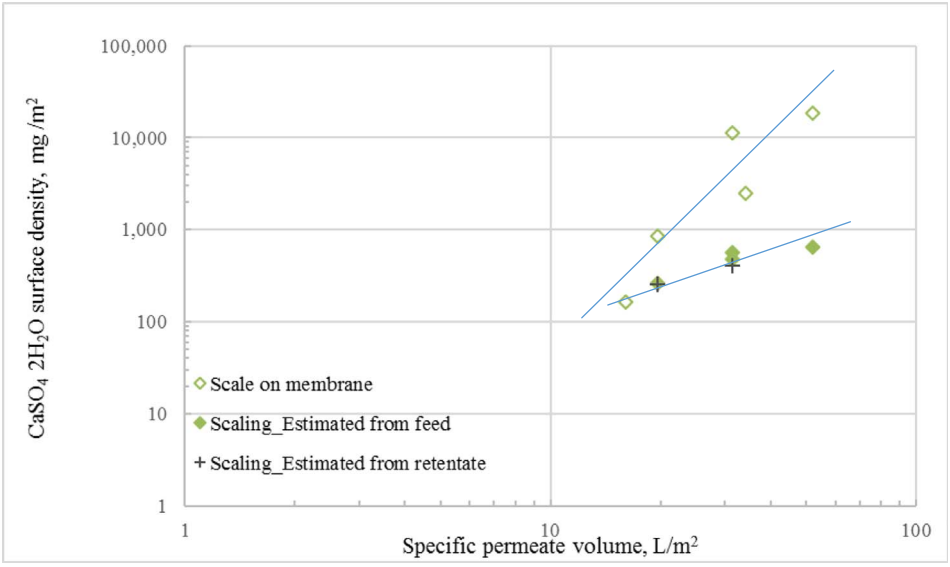

Fig. 9. *Scaling in the absence of alginate*. Comparison of gypsum surface density on the desalination membrane with equivalent deposit density corresponding to filtration of feed and retentate solution.

matter pre-deposited on the membrane) corresponds to greater deposited $CaSO_4$ mass than that corresponding to the higher SA foulant concentration (10 mg/L, tests 123, 144, 150); i.e. the greater pre-deposited polysaccharide mass on the membrane is associated with a reduced $CaSO_4$ deposit. The exact cause of this effect is unclear. For instance, invoking "cake enhanced concentration polarization - CEOP" [54] one may reach a conclusion contrary to the experimentally observed trend; indeed, CEOP is considered to lead to increased concentration of rejected species near the membrane (and plausibly to greater Ca-species supersaturation), which should lead to increased membrane scaling for thicker fouling layers (i.e. case of 10 mg/L) – contrary to the present experimental result. Only the limited data points at specific volume ~15 L/m^2 seem to follow this trend, although possible experimental error renders this observation uncertain.

It is also of interest to assess the data from dissolution and analysis of precipitates on the 0.2 μm membrane (from filtration of retentate and stagnant feed solution, Table S2, Supplement) with corresponding data on scaling during desalination. Fig. 9 shows a comparison of gypsum surface density on the desalination membrane with corresponding *equivalent deposit density* estimated via filtration of feed and retentate solution and determination of calcium, with no alginates present. In Fig. 9 and Table S2 (Supplement), the equivalent deposit density from feed or retentate solution (of the same "age" as the duration of a corresponding desalination test) is estimated by considering *filtration of the same specific permeate volume* as the corresponding desalination test. It is evident that the rate of $CaSO_4$ precipitation in bulk solution (whether retentate under agitation or stagnant feed batch) is much smaller compared to the rate of membrane scaling during desalination; the same qualitative conclusion can be drawn from the SEM pictures (Figs. 3 to 6) as discussed in foregoing section.

These new data lend significant direct support to the mechanism whereby membrane scaling is primarily due to growth of "surface particles", which originate from surface nuclei and tiny nuclei/particles depositing from the retentate bulk; the direct contribution of the latter to membrane scaling is apparently small. This result has already been presented and discussed in previous publications from the authors' laboratory (e.g. [17,55]). It should be added that for the scaling tests in the presence of alginates, the difference in the rate of solid $CaSO_4$ growth on the membrane surface (scaling) compared to that in the supersaturated solution bulk is significantly smaller due to the aforementioned strong inhibition action of the polysaccharide, as shown in the respective data included in Tables S1 and S2, Supplement.

Despite the value of the scale-deposit data presented in this section, their quantity is insufficient to determine percent error involved. This is due to quite a few common sources of error existing in the sequence of experimental steps, between feed-solution preparation and final membrane-sample treatment (scale dissolution and analyses), that lead to the finally computed scale membrane-surface density (in mg/m^2). Significant sources of error also exist in the main filtration/desalination test, including variation of flux and of permeability of membrane specimens. For instance, as shown in Table A1, an effort to replicate data for scaling (Runs #94 and #95) and combined fouling/scaling (Runs #131 and #148), by using practically the same feed-fluid composition and test conditions, has led to differences in the results plotted in Fig. 7b even though the general trend is clear. For this reason, lines drawn through the data, in this and other figures, merely indicate trends; moreover, percentage error determination of deposit surface density (and correlation of scaling rates with key process parameters) requires a sufficiently large database.

4.4. Discussion

An effort was made in the present dead-end tests to create well-controlled conditions, close to those prevailing in brackish-water desalination SWM modules where scaling potential tends to develop. Therefore, as noted in foregoing sections, appropriate fluid composition (including Ca concentration), mean permeation flux (ca. 14 L/m^2 h), fluid agitation rate (creating mean wall shear stress typical of that prevailing in spacer filled channels) were selected in order to obtain conditions similar to those existing in tail SWM modules where supersaturation first develops. The small initial supersaturation ratio (S ~ 1.4) remained practically constant during the experiments, since the pressurized fluid volume in the test-cell was kept constant (through an auxiliary deionized water vessel, Fig. 1) and the precipitated $CaSO_4$ was insignificant compared to the calcium inventory in the agitated filtration cell. Additionally, the employed small alginate concentration was realistic for the problem studied.

Considering the well-documented complexation of Ca^{2+} ions with the negatively charged carboxylate group [COO^-] of alginates, it is necessary to estimate the concentration/availability of free Ca^{2+} when alginates are mixed in the weakly supersaturated solution. Based on the data presented in [56], it is estimated that the maximum uptake capacity of Ca^{2+} ions by alginates is roughly *2.5 mM·Ca^{2+} per gram of dry mass of alginic acid*. Using, for estimation purposes, a conservative solution concentration of 10 mg alginic acid per L, the maximum uptake capacity of Ca^{2+} ions by alginates is insignificant (of order 10^{-2} mM·Ca^{2+}) compared to the available ~35 mM·Ca^{2+} in the feed solution of present tests. Moreover, Siew et al. [57] have shown that the maximum binding capacity of Ca^{2+} is ~0.33 M [Ca^{2+}] per M [COO^-]. Considering a typical molecular structure of alginic acid and the likely modes of Ca-binding [58], this figure confirms the preceding estimate of maximum [Ca^{2+}] uptake by the alginates. The implication of this observation is that Ca-alginate complexation in the bulk solution does not affect Ca^{2+} ion availability and feed-solution supersaturation; therefore, the dominant mechanism of $CaSO_4$ threshold and/or crystal growth inhibition may be related to the blocking by alginate macromolecules of nuclei and/or of developing crystal active sites (e.g. [36,52]). It is of interest to note that Lee et al. [25] investigating $CaSO_4$ scaling in the presence of humic acid (HA) reached a similar conclusion, by considering the calcium binding capacity of HA; i.e. that calcium complexation has insignificant direct effect on scale formation. Also the crystal habit in presence of HA is prismatic, instead of elongated, as observed in tests with 2 mg/L·SA in this study (Fig. 4a).

It should be pointed out that there is ample evidence in the literature on the capability of alginates for inhibition of sparingly salts crystallization, which is in support of the new results reported herein. McCartney and Alexander [35] established that polymers containing carboxyl groups (such as alginic acid, polyacrylie acid and other) were particularly effective inhibitors of calcium sulfate crystallization. On the mechanism, Smith and Alexander [52] suggested that such adsorbed polymer molecules acted as immobile impurities on the crystal surface, thus inhibiting crystal growth by reducing the rate of step movement across the crystal surface. Manoli and Dalas [59] studied $CaCO_3$ crystal growth retardation by SA, and recently Lakshtanov et al. [60] inhibition and interaction mechanisms of SA regarding calcite growth and recrystallization. Malkaj et al. [61] obtained strong crystal growth rate reduction of hydroxyapatite by SA, attributed to inhibitor adsorption onto the active growth sites. In an interesting recent study of brushite crystallization inhibition in the presence of alginates Ucar et al. [62] reported evidence that crystal-growth retardation was most pronounced when the G-block (comprising the alginates) was present in the solution. These results are supported by the work of Giuffre et al. [63] who presented experimental evidence that, for the case of calcium carbonate nucleation in a substrate of polysaccharides (PS), thermodynamic barriers to nucleation are significantly affected by the type of PS molecular structure; specifically, they have shown that the highest energy barriers to calcite nucleation were correlated with the charge-dense constituent of alginates (i.e. the low-guluronic-acid, LG) com-

pared to a relatively low energy barrier for nucleation onto a chitosan substrate. Finally, of interest in respect of membrane water treatment applications is the work of Reddy and Hoch [64] on calcite crystal growth rate inhibition affected by aquatic humic substances, frequently encountered in feed-waters.

5. Conclusions

This experimental study was performed in a dead-end pressurized filtration cell under well-controlled conditions, mimicking those prevailing in the tail elements of pressure vessels of brackish water desalination plants where calcium salts supersaturation appears. During all tests, practically *constant supersaturation* was maintained in the bulk of filtered fluid. For each test in the presence of alginates (either mixed in the feed fluid or pre-deposited on the membrane), a companion desalination/scaling test was also performed under exactly the same conditions but without alginate, as a reference. Incipient calcium sulfate membrane scaling and precipitation were studied over a test period extending to 240 min. Membrane scale and bulk precipitates were characterized by Scanning Electron Microscopy and quantified via sample dissolution and analysis.

The reference tests exhibited a fairly strong rate of membrane scaling by calcium sulfate, despite the rather small bulk supersaturation ratio ($S \sim 1.4$) and the significant wall shear stresses (imposed by agitation) that tend to reduce concentration polarization. On the contrary, the rate of calcium sulfate precipitation in the bulk (of both agitated retentate and stagnant feed-solution) was much smaller. This difference is attributed to the mechanism of membrane scaling during desalination, involving mainly "surface nuclei/crystallite" growth enhanced by the increased supersaturation and mass transfer coefficient at the membrane surface, as has already been observed and discussed (e.g. [17,55]). Flux reduction in these tests, observed only after significant membrane coverage by the typical elongated gypsum crystals, was in accord with similar previous observations (e.g. [48]).

The presence of alginates in the supersaturated solution (at 2 mg/L and 10 mg/L·SA concentration) resulted in *quite strong inhibition* of membrane scaling; this effect was stronger at the higher alginate concentration, and the mechanism appeared to be that of "threshold inhibition" [53]. Under these test conditions, tiny amorphous plate-like $CaSO_4$ particles were observed to grow inside the alginate fouling layer on the membrane. Moreover, in the presence of 10 mg/L SA, the estimated deposits mass surface density on the membrane (obtained through solids dissolution) was more than one order of magnitude smaller than that of the alginate-free solution, for the same fluid desalination period; nevertheless, the rate of increase of deposit-mass surface density appeared to be significant over the period tested. Similar inhibition of precipitation was observed in the agitated retentate bulk as well as in the stagnant feed solution. The effect of membrane fouling on flux reduction appeared to be significant only in the initial period of filtration, with a tendency to reach a nearly steady flux level thereafter; this flux stabilization may be attributed to the imposed significant shear stress that may have led to a nearly constant fouling layer. No significant change in ionic species rejection was observed in these tests.

The results of scaling experiments in the presence of smaller alginate concentration (2 mg/L SA) were generally similar to those outlined above, although the inhibition effect was weaker as shown by the dissolution tests. A "crystal growth-retardation" type of inhibition effect (e.g. [63]) was identified in some tests. In addition to reduced deposit-mass surface density (compared to reference scaling tests), this type of inhibition was characterized by significant crystal habit modification (of the typical elongated particles) to prismatic shapes; the latter were also observed in similar $CaSO_4$ studies with other inhibitors [36]. The significant inhibition effect was also evident in the meager amount of precipitates filtered out of the agitated retentate and the stagnant feed solution, as in the case with greater alginate concentration. However, insignificant effect of combined fouling-scaling was observed in this case on flux reduction and membrane salt rejection, compared to reference.

In the case of desalination through a membrane pretreated with a dilute alginate-foulant solution, scale inhibition was also observed, in comparison with the reference no-alginate tests. However, this effect was somewhat weaker compared to the case of desalination with alginates present in the feed solution. The inhibition effect was evident in both the reduced deposit-mass surface density and the solid/crystal particle shapes; specifically, tiny amorphous flat particles as well as rosette type deposits were identified in the fouling layer, qualitatively similar to those of previous studies (e.g. [22]).

Regarding the inhibition mechanism, the gel-type alginate fouling layers and possibly alginate agglomerates developing in the bulk [50] may play a significant role, in addition to the basic role played by the carboxylic groups which tend to block active sites of growing nuclei/crystallites (e.g. [52]). More research over a broader range of conditions is required to clarify these issues, and to obtain correlations, of membrane scaling rate with feed-fluid composition, of practical use.

Acknowledgements

The authors wish to thank the personnel of Analytical Services Unit of the Chemical Process and Energy Resources Institute, Centre for Research and Technology Hellas (ASU-CPERI-CERTH) for analytical support.

Appendix A

A comprehensive Table A1 includes the experimental conditions and main parameters of all the tests performed in this study. Data from inorganic and organic fouling layer dissolution tests, feedwater and retentate characteristics and SEM images (from fouled desalination membranes and 0.2 μm membrane filters) are included in Appendix B (Supplementary data).

Table A1
Composition of feed solutions, conditions and key parameter values of various tests performed in this study. Test ID numbers appear in the top row; the second row (in parentheses) indicates the companion test ran simultaneously in the second cell, under the same conditions, but with different fluid composition for comparison.

Feed water	Scaling tests						Combined fouling/scaling tests							Scaling after fouling tests					Fouling tests				
	94 (95)	95 (94)	145 (146)	134 (133)	146 (145)	130 (129)	128	133 (134)	131	148 (147)	129 (130)	137	147 (148)	123 (124)	150 (149)	149 (150)	142 (141)	144 (143)	140 (139)	141 (142)	124 (123)	139 (140)	143 (144)
Ca^{2+}, mM	32.6	32.6	32.7	34.8	32.7	34.6	34.4	34.4	34.8	34.8	34.8	32.9	34.2	34.0	34.4	34.4	34.0	33.5	2.0	2.0	2.0	2.0	1.9
SO_4^{2-}, mM	35.0	35.0	39.0	27.6	39.5	28.4	35.6	28.3	31.7	34.3	28.7	38.0	33.1	32.4	38.8	38.8	35.2	37.9	–	37.9	–	–	32.6
Na^+, mM	70.0	70.0	78.1	55.2	78.1	56.8	71.1	56.6	63.3	68.6	57.3	76.0	66.1	64.9	77.6	77.6	70.3	75.7	–	75.0	–	–	ND
Cl^-, mM	72.5	72.5	71.1	69.6	71.1	79.6	73.3	72.8	71.7	70.4	84.1	70.3	71.2	59.7	68.8	68.8	70.7	72.0	ND	ND	ND	ND	ND
SA, mg/L	–	–	–	–	–	–	2	2	2	2	10	10	10	[10]	[10]	[10][a]	[2]	[10]	2	2	10	10	10
eC, μS/cm	10,970	10,970	11,220	10,630	11,220	10,651	10,640	10,645	10,520	11,250	10,665	11,040	11,270	10,580	11,260	11,260	11,090	11,090	496	5640	453	495	6510
Osmotic pressure, psi	72	72	74	62	74	66	72	64	67	65	68	72	68	63	73	73	70	73	2	40	2	2	35
Rejection, %	97.1	98.4	97.2	97.3	97.8	98.3	98.6	96.3	98.1	97	97.8	98.0	98.6	98.6	96	98	98.2	97.9	98.2	99.7	96.7	98.2	99.0
S	1.43	1.43	1.48	1.36	1.48	1.36	1.46	1.36	1.43	1.46	1.36	1.46	1.45	1.43	1.50	1.50	1.45	1.48	–	–	–	–	–
S_w	1.50	1.50	1.55	1.46	1.55	1.45	1.55	1.46	1.50	1.53	1.46	1.55	1.53	1.50	1.58	1.58	1.53	1.55	–	–	–	–	–
pH	5.9	5.9	6.0	5.7	6.0	5.6	5.7	5.7	5.8	5.5	5.7	5.9	5.5	5.7	5.8	5.8	5.9	6.2	6.2	5.9	5.6	6.2	6.0
Duration, min	90	90	90	120	180	240	90	120	240	240	240	240	300	90	240	240	240	240	240	240	100	240	240
Permeate volume, ml	14.6	14.6	17.8	31.0	28.5	47.4	20.9	27.8	47.6	46.5	51.2	48.7	61.5	12.2	41.6	46.8	47.6	47.6	87.2	68.6	30.0	81.1	72.3
ΔP_{ap}, psi	150	150	170	170	170	170–1-60	170	170	170	170	170	170	170	150	170	170	170	170	170	170	150	170	170
Flux, L/m^{2}h	10.6	10.9	13	16.7	10.6	16.7–1-3.2	14.9	15.2	12.9	12.8	14.1	13.5	13.5	8.9	11.7	12.9	13.0	13.2	23.8	18.7	19.7	24–20	19.6

ND: Not determined.
[a] Without agitation.

Appendix B. Supplementary data

Supplementary data to this article can be found online at http://dx.doi.org/10.1016/j.desal.2017.04.009.

References

[1] M. Wilf, (contributors L. Awerbuch, C. Bartels, M. Mickley, G. Pearce, N. Voutchkov), The Guidebook to Membrane Desalination Technology, Balaban Desalination Publications, 2007.

[2] X.-M. Wang, T.D. Waite, Impact of gel layer formation on colloid retention in membrane filtration processes, J. Membr. Sci. 325 (2008) 486–494, http://dx.doi.org/10.1016/j.memsci.2008.08.016.

[3] K. Katsoufidou, S.G. Yiantsios, A.J. Karabelas, Experimental study of ultrafiltration membrane fouling by sodium alginate and flux recovery by backwashing, J. Membr. Sci. 300 (2007) 137–146, http://dx.doi.org/10.1016/j.memsci.2007.05.017.

[4] E. Ferrero, S. Navea, C. Repolles, J. Bacardit, J. Malfeito, Analytical methods for the characterization of Reverse Osmosis membrane fouling, IDA World Congress Proceedings, Paper IDAWC/PER11-240, Sept. 4–9 2011.

[5] M.D. McCarthy, J.I. Hedges, R. Benner, The chemical composition of dissolved organic matter in seawater, Chem. Geol. 107 (1993) 503–507, http://dx.doi.org/10.1016/0009-2541(93)90240-J.

[6] S. Shirazi, C.-J. Lin, D. Chen, Inorganic fouling of pressure-driven membrane processes - a critical review, Desalination 250 (2010) 236–248, http://dx.doi.org/10.1016/j.desal.2009.02.056.

[7] R.Y. Ning, Reverse osmosis process chemistry relevant to the Gulf, Desalination 123 (1999) 157–164, http://dx.doi.org/10.1016/S0011-9164(99)00069-7.

[8] C.Y. Tang, T.H. Chong, A.G. Fane, Colloidal interactions and fouling of NF and RO membranes: a review, Adv. Colloid Interf. Sci. 164 (2011) 126–143, http://dx.doi.org/10.1016/j.cis.2010.10.007.

[9] W.S. Ang, A. Tiraferri, K.L. Chen, M. Elimelech, Fouling and cleaning of RO membranes fouled by mixtures of organic foulants simulating wastewater effluent, J. Membr. Sci. 376 (2011) 196–206, http://dx.doi.org/10.1016/j.memsci.2011.04.020.

[10] A.J. Karabelas, D.C. Sioutopoulos, New insights into organic gel fouling of reverse osmosis desalination membranes, Desalination 368 (2015) 114–126, http://dx.doi.org/10.1016/j.desal.2015.01.029.

[11] D. Hasson, Precipitation fouling, in: E.F.C. Somerscales, J.G. Knudsen (Eds.), Fouling of Heat Transfer Equipment, Hemisphere Pub. Corp, Washington, D.C., 1981, pp. 527–568 (https://books.google.gr/books?id=wd5SAAAAMAAJ).

[12] N. Andritsos, M. Kontopoulou, A.J. Karabelas, P.G. Koutsoukos, Calcium carbonate deposit formation under isothermal conditions, Can. J. Chem. Eng. 74 (1996) 911–919, http://dx.doi.org/10.1002/cjce.5450740614.

[13] J. Gilron, D. Hasson, Calcium sulphate fouling of reverse osmosis membranes: flux decline mechanism, Chem. Eng. Sci. 42 (1987) 2351–2360 (http://www.scopus.com/inward/record.url?eid=2-s2.0-).

[14] W.-Y. Shih, A. Rahardianto, R.-W. Lee, Y. Cohen, Morphometric characterization of calcium sulfate dihydrate (gypsum) scale on reverse osmosis membranes, J. Membr. Sci. 252 (2005) 253–263, http://dx.doi.org/10.1016/j.memsci.2004.12.023.

[15] A. Antony, J.H. Low, S. Gray, A.E. Childress, P. Le-Clech, G. Leslie, Scale formation and control in high pressure membrane water treatment systems: a review, J. Membr. Sci. 383 (2011) 1–16, http://dx.doi.org/10.1016/j.memsci.2011.08.054.

[16] M. Kostoglou, A.J. Karabelas, On modeling incipient crystallization of sparingly soluble salts in frontal membrane filtration, J. Colloid Interface Sci. 362 (2011) 202–214, http://dx.doi.org/10.1016/j.jcis.2011.06.040.

[17] A.J. Karabelas, A. Karanasiou, S.T. Mitrouli, Incipient membrane scaling by calcium sulfate during desalination in narrow spacer-filled channels, Desalination 345 (2014) 146–157, http://dx.doi.org/10.1016/j.desal.2014.04.020.

[18] T. Tran, B. Bolto, S. Gray, M. Hoang, E. Ostarcevic, An autopsy study of a fouled reverse osmosis membrane element used in a brackish water treatment plant, Water Res. 41 (2007) 3915–3923, http://dx.doi.org/10.1016/j.watres.2007.06.008.

[19] M.T. Khan, C.-L.d.O. Manes, C. Aubry, J.-P. Croué, Source water quality shaping different fouling scenarios in a full-scale desalination plant at the Red Sea, Water Res. 47 (2013) 558–568, http://dx.doi.org/10.1016/j.watres.2012.10.017.

[20] E.M.V. Hoek, J. Allred, T. Knoell, B.-H. Jeong, Modeling the effects of fouling on full-scale reverse osmosis processes, J. Membr. Sci. 314 (2008) 33–49, http://dx.doi.org/10.1016/j.memsci.2008.01.025.

[21] Y.L. Hou, J.X. Li, Y.N. Gao, X.C. Xu, Y. Cai, N. Yang, Monitoring of CaSO4 deposition behaviors on biofilm during nanofiltration via ultrasonic time-domain reflectometry (UTDR), Water Sci. Technol. 61 (2010) 2853–2861, http://dx.doi.org/10.2166/wst.2010.165.

[22] J. Thompson, N. Lin, E. Lyster, R. Arbel, T. Knoell, J. Gilron, Y. Cohen, RO membrane mineral scaling in the presence of a biofilm, J. Membr. Sci. 415–416 (2012) 181–191, http://dx.doi.org/10.1016/j.memsci.2012.04.051.

[23] Y. Liu, B. Mi, Effects of organic macromolecular conditioning on gypsum scaling of forward osmosis membranes, J. Membr. Sci. 450 (2014) 153–161, http://dx.doi.org/10.1016/j.memsci.2013.09.001.

[24] J. Wang, L. Wang, R. Miao, Y. Lv, X. Wang, X. Meng, R. Yang, X. Zhang, Enhanced gypsum scaling by organic fouling layer on nanofiltration membrane: characteristics and mechanisms, Water Res. 91 (2016) 203–213, http://dx.doi.org/10.1016/j.watres.2016.01.019.

[25] S. Lee, J.-S. Choi, C.-H. Lee, Behaviors of dissolved organic matter in membrane desalination, Desalination 238 (2009) 109–116, http://dx.doi.org/10.1016/j.desal.2008.01.041.

[26] K.S. Anseth, C.N. Bowman, L. Brannon-Peppas, Mechanical properties of hydrogels and their experimental determination, Biomaterials 17 (1996) 1647–1657, http://dx.doi.org/10.1016/0142-9612(96)87644-7.

[27] I. Donati, S. Paoletti, Material properties of alginates, in: B.H.A. Rehm (Ed.), Alginates: Biology and Applications, Springer Berlin Heidelberg, Berlin, Heidelberg, 2009, pp. 1–53, , http://dx.doi.org/10.1007/978-3-540-92679-5_1.

[28] G.T. Grant, E.R. Morris, D.A. Rees, P.J.C. Smith, D. Thom, Biological interactions between polysaccharides and divalent cations: the egg-box model, FEBS Lett. 32 (1973) 195–198, http://dx.doi.org/10.1016/0014-5793(73)80770-7.

[29] A.G. Kalinichev, E. Iskrenova-Tchoukova, W.-Y. Ahn, M.M. Clark, R.J. Kirkpatrick, Effects of Ca2 + on supramolecular aggregation of natural organic matter in aqueous solutions: a comparison of molecular modeling approaches, Geoderma 169 (2011) 27–32, http://dx.doi.org/10.1016/j.geoderma.2010.09.002.

[30] D.C. Sioutopoulos, T.B. Goudoulas, E.G. Kastrinakis, S.G. Nychas, A.J. Karabelas, Rheological and permeability characteristics of alginate fouling layers developing on reverse osmosis membranes during desalination, J. Membr. Sci. 434 (2013) 74–84, http://dx.doi.org/10.1016/j.memsci.2013.01.018.

[31] Y. Xiang, Y. Liu, B. Mi, Y. Leng, Hydrated polyamide membrane and its interaction with alginate: a molecular dynamics study, Langmuir 29 (2013) 11600–11608, http://dx.doi.org/10.1021/la401442r.

[32] Y. Xiang, Y. Liu, B. Mi, Y. Leng, Molecular dynamics simulations of polyamide membrane, calcium alginate gel, and their interactions in aqueous solution, Langmuir 30 (2014) 9098–9106, http://dx.doi.org/10.1021/la501811d.

[33] Y. Mo, A. Tiraferri, N.Y. Yip, A. Adout, X. Huang, M. Elimelech, Improved antifouling properties of polyamide Nanofiltration membranes by reducing the density of surface carboxyl groups, Environ. Sci. Technol. 46 (2012) 13253–13261, http://dx.doi.org/10.1021/es303673p.

[34] J. Wu, A.E. Contreras, Q. Li, Studying the impact of RO membrane surface functional groups on alginate fouling in seawater desalination, J. Membr. Sci. 458 (2014) 120–127, http://dx.doi.org/10.1016/j.memsci.2014.01.056.

[35] E.R. McCartney, A.E. Alexander, The effect of additives upon the process of crystallization, J. Colloid Sci. 13 (1958) 383–396, http://dx.doi.org/10.1016/0095-8522(58)90047-3.

[36] M.G. Lioliou, C.A. Paraskeva, P.G. Koutsoukos, A.C. Payatakes, Calcium sulfate precipitation in the presence of water-soluble polymers, J. Colloid Interface Sci. 303 (2006) 164–170, http://dx.doi.org/10.1016/j.jcis.2006.07.054.

[37] J.W. Mullin, 3 - Solutions and Solubility, in: Crystallization, (Fourth edition), Butterworth-Heinemann, Oxford, 2001, pp. 86–134, http://dx.doi.org/10.1016/B978-075064833-2/50005-X.

[38] J. MacAdam, P. Jarvis, Chapter 1 - Water-formed scales and deposits: types, characteristics, and relevant industries A2, in: Zahid Amjad, K.D. Demadis (Eds.), Mineral Scales and Deposits, Elsevier, Amsterdam, 2015, pp. 3–23, , http://dx.doi.org/10.1016/B978-0-444-63228-9.00001-2.

[39] D.L. Parkhurst, C.A.J. Appelo, User's guide to PHREEQC (Version 2): a computer program for speciation, batch-reaction, one-dimensional transport, and inverse geochemical calculations, U.S. Geological Survey, Earth Science Information Center, 1999Open-File Reports Section [distributor].

[40] M. Mulder, Basic Principles of Membrane Technology, Springer, Netherlands, 1996, http://dx.doi.org/10.1007/978-94-009-1766-8.

[41] C.P. Koutsou, A.J. Karabelas, Shear stresses and mass transfer at the base of a stirred filtration cell and corresponding conditions in narrow channels with spacers, J. Membr. Sci. 399–400 (2012) 60–72, http://dx.doi.org/10.1016/j.memsci.2012.01.029.

[42] J.M.M. Peeters, J.P. Boom, M.H.V. Mulder, H. Strathmann, Retention measurements of nanofiltration membranes with electrolyte solutions, J. Membr. Sci. 145 (1998) 199–209, http://dx.doi.org/10.1016/S0376-7388(98)00079-9.

[43] S. Mitrouli, A.J. Karabelas, A. Karanasiou, M. Kostoglou, Incipient calcium carbonate scaling of desalination membranes in narrow channels with spacers—experimental insights, J. Membr. Sci. 425–426 (2013) 48–57, http://dx.doi.org/10.1016/j.memsci.2012.09.025.

[44] D.C. Sioutopoulos, A.J. Karabelas, Correlation of organic fouling resistances in RO and UF membrane filtration under constant flux and constant pressure, J. Membr. Sci. 407–408 (2012) 34–46, http://dx.doi.org/10.1016/j.memsci.2012.03.036.

[45] L.S. Clescheri, A.E. Greenberg, R.R. Trussell, Standard methods for the examination of water and wastewater, American Public Health Association, American Water Works Association, Water Pollution Control Federation, Washington, 1989.

[46] S.T. Mitrouli, A.J. Karabelas, N.P. Isaias, Polyamide active layers of low pressure RO membranes: data on spatial performance non-uniformity and degradation by hypochlorite solutions, Desalination 260 (2010) 91–100, http://dx.doi.org/10.1016/j.desal.2010.04.061.

[47] A.J. Karabelas, M. Kostoglou, S.T. Mitrouli, Incipient crystallization of sparingly soluble salts on membrane surfaces: the case of dead-end filtration with no agitation, Desalination 273 (2011) 105–117, http://dx.doi.org/10.1016/j.desal.2010.10.057.

[48] C. Tzotzi, T. Pahiadaki, S.G. Yiantsios, A.J. Karabelas, N. Andritsos, A study of CaCO3 scale formation and inhibition in RO and NF membrane processes, J. Membr. Sci. 296 (2007) 171–184, http://dx.doi.org/10.1016/j.memsci.2007.03.031.

[49] D.C. Sioutopoulos, A.J. Karabelas, Evolution of organic gel fouling resistance in constant pressure and constant flux dead-end ultrafiltration: differences and similarities, J. Membr. Sci. 511 (2016) 265–277, http://dx.doi.org/10.1016/j.memsci.2016.03.057.
[50] Y. Mo, K. Xiao, Y. Shen, X. Huang, A new perspective on the effect of complexation between calcium and alginate on fouling during nanofiltration, Sep. Purif. Technol. 82 (2011) 121–127, http://dx.doi.org/10.1016/j.seppur.2011.08.033.
[51] S.-T. Liu, G.H. Nancollas, The crystal growth of calcium sulfate dihydrate in the presence of additives, J. Colloid Interface Sci. 44 (1973) 422–429, http://dx.doi.org/10.1016/0021-9797(73)90318-4.
[52] B.R. Smith, A.E. Alexander, The effect of additives on the process of crystallization II. Further studies on calcium sulphate (1), J. Colloid Interface Sci. 34 (1970) 81–90, http://dx.doi.org/10.1016/0021-9797(70)90261-4.
[53] K.G. Cooper, L.G. Hanlon, G.M. Smart, R.E. Talbot, The threshold scale inhibition phenomenon, Desalination 31 (1979) 257–266, http://dx.doi.org/10.1016/S0011-9164(00)88526-4.
[54] E.M.V. Hoek, M. Elimelech, Cake-enhanced concentration polarization: a new fouling mechanism for salt-rejecting membranes, Environ. Sci. Technol. 37 (2003) 5581–5588, http://dx.doi.org/10.1021/es0262636.
[55] S.T. Mitrouli, M. Kostoglou, A.J. Karabelas, A. Karanasiou, Incipient crystallization of calcium carbonate on desalination membranes: dead-end filtration with agitation, Desalin. Water Treat. 57 (2016) 2855–2869, http://dx.doi.org/10.1080/19443994.2014.990931.
[56] C. Jeon, J.Y. Park, Y.J. Yoo, Characteristics of metal removal using carboxylated alginic acid, Water Res. 36 (2002) 1814–1824, http://dx.doi.org/10.1016/S0043-1354(01)00389-X.
[57] C.K. Siew, P.A. Williams, N.W.G. Young, New insights into the mechanism of gelation of alginate and pectin: charge annihilation and reversal mechanism, Biomacromolecules 6 (2005) 963–969, http://dx.doi.org/10.1021/bm049341l.
[58] N. Emmerichs, J. Wingender, H.C. Flemming, C. Mayer, Interaction between alginates and manganese cations: identification of preferred cation binding sites, Int. J. Biol. Macromol. 34 (2004) 73–79, http://dx.doi.org/10.1016/j.ijbiomac.2004.03.004.
[59] F. Manoli, E. Dalas, The effect of sodium alginate on the crystal growth of calcium carbonate, J. Mater. Sci. Mater. Med. 13 (2002) 155–158, http://dx.doi.org/10.1023/a:1013825912150.
[60] L.Z. Lakshtanov, D.A. Belova, D.V. Okhrimenko, S.L.S. Stipp, Role of alginate in calcite recrystallization, Cryst. Growth Des. 15 (2015) 419–427, http://dx.doi.org/10.1021/cg501492c.
[61] P. Malkaj, E. Pierri, E. Dalas, The crystallization of hydroxyapatite in the presence of sodium alginate, J. Mater. Sci. Mater. Med. 16 (2005) 733–737, http://dx.doi.org/10.1007/s10856-005-2610-9.
[62] S. Ucar, S.H. Bjørnøy, D.C. Bassett, B.L. Strand, P. Sikorski, J.-P. Andreassen, Nucleation and growth of Brushite in the presence of alginate, Cryst. Growth Des. 15 (2015) 5397–5405, http://dx.doi.org/10.1021/acs.cgd.5b01032.
[63] A.J. Giuffre, L.M. Hamm, N. Han, J.J. De Yoreo, P.M. Dove, Polysaccharide chemistry regulates kinetics of calcite nucleation through competition of interfacial energies, Proc. Natl. Acad. Sci. 110 (2013) 9261–9266.
[64] M.M. Reddy, A.R. Hoch, Calcite crystal growth rate inhibition by aquatic humic substances, in: Z. Amjad (Ed.), Advances in Crystal Growth Inhibition Technologies, Springer US, Boston, MA, 2002, pp. 107–121, , http://dx.doi.org/10.1007/0-306-46924-3_8.